Electrical investigation of the oblique Hanle effect in ferromagnet/oxide/semiconductor contacts

Kun-Rok Jeon,[1,2] Byoung-Chul Min,[3] Youn-Ho Park,[3] Seung-Young Park,[4] and Sung-Chul Shin[1,5,*]

[1]*Department of Physics and Center for Nanospinics of Spintronic Materials, Korea Advanced Institute of Science and Technology (KAIST), Daejeon 305-701, Korea*

[2]*National Institute of Advanced Industrial Science and Technology (AIST), Spintronics Research Center, Tsukuba, Ibaraki 305-8568, Japan*

[3]*Center for Spintronics Research, Korea Institute of Science and Technology (KIST), Seoul 136-791, Korea*

[4]*Division of Materials Science, Korea Basic Science Institute (KBSI), Daejeon 305-764, Korea*

[5]*Department of Emerging Materials Science, Daegu Gyeongbuk Institute of Science and Technology (DGIST), Daegu 711-873, Korea*

(Received 8 January 2013; revised manuscript received 8 April 2013; published 22 May 2013)

We have investigated the electrical Hanle effect with magnetic fields applied at an oblique angle (θ) to the spin direction [the oblique Hanle effect (OHE)] in CoFe/MgO/semiconductor (SC) contacts by employing a three-terminal measurement scheme. The electrical oblique Hanle signals obtained in CoFe/MgO/Si and CoFe/MgO/Ge contacts show clearly different line shapes depending on the spin lifetime of the host SC. Notably, at moderate magnetic fields, the asymptotic values of the oblique Hanle signals (in both contacts) are consistently reduced by a factor of $\cos^2(\theta)$ irrespective of the bias current and temperature. These results are in good agreement with predictions of the spin precession and relaxation model for the electrical OHE. At high magnetic fields where the magnetization of CoFe is significantly tilted from the film plane to the magnetic-field direction, we find that the observed angular dependence of voltage signals in the CoFe/MgO/Si and CoFe/MgO/Ge contacts is well explained by the OHE, considering the misalignment angle between the external magnetic field and the magnetization of CoFe.

DOI: 10.1103/PhysRevB.87.195311 PACS number(s): 72.25.Dc, 72.25.Mk, 75.47.−m, 85.75.−d

I. INTRODUCTION

The electrical injection of spin-polarized electrons from a ferromagnet (FM) into a semiconductor (SC) and the subsequent detection of the resultant spin accumulation are the major building blocks of SC-based spintronics.[1–5] By engineering ferromagnetic tunnel contacts, the electrical injection and detection of the spin accumulation in various SC systems have been demonstrated up to room temperature (RT) through the Hanle effect.[4,5]

The approach based on the Hanle effect,[6,7] in which a magnetic field transverse to the spins suppresses the spin accumulation in a SC via spin precession and dephasing, provides an unambiguous means to establish the presence of spin accumulation in a SC. In particular, the oblique Hanle effect [i.e., the Hanle effect in an oblique magnetic field (OHE)][6–10] enables us to obtain additional information of spin dynamics and convincing proof of spin accumulation in the SC. The optical OHE using an optical detection technique (or the circular polarization of emitted light) in SC[8–11] has been intensely studied in spin light-emitting diodes (spin LEDs). However, the counterpart of the electrical OHE in SC still needs to be explored.[6,7,12,13]

Here, we report the electrical investigation of the OHE in FM/oxide/SC contacts and their generic features using a three-terminal measurement scheme. The electrical OHE signals obtained in CoFe/MgO/Si and CoFe/MgO/Ge contacts show clearly different features depending on the spin relaxation time of the host SC. Notably, their asymptotic values (in both contacts) are consistently reduced by a factor of $\cos^2(\theta)$ in moderate magnetic fields at an oblique angle (θ) to the spin direction irrespective of the bias current (I) and temperature (T). These results are highly consistent with predictions of the spin precession and relaxation model for the electrical OHE. The angular dependence of voltage signals obtained at high magnetic fields where the magnetization of CoFe is significantly tilted from the film plane to the magnetic field direction is also well explained by the same model, taking into account the misalignment angle between the external magnetic field and the magnetization of CoFe.

II. EXPERIMENTAL DETAILS

A. Device fabrication

Two types of CoFe(5 nm)/MgO(2 nm)/n−type SC(001) tunnel contacts were prepared using a molecular-beam-epitaxy system. The first type is a highly textured CoFe/MgO/Si contact [Fig. 1(a)] in which the Si channel is heavily As-doped ($n_d \sim 2.5 \times 10^{19}$ cm^{-3} at 300 K),[14] and the second is a single-crystalline CoFe/MgO/Ge contact [Fig. 1(b)] in which the Ge channel consists of a heavily P-doped surface layer ($n_d \sim 10^{19}$ cm^{-3} at 300 K) and a moderately Sb-doped substrate ($n_d \sim 10^{18}$ cm^{-3} at 300 K).[14] All layers were deposited by electron-beam (e-beam) evaporation with a working pressure better than 2×10^{-9} Torr. The MgO film was deposited from an MgO single-crystal source with a deposition rate of ∼0.17 nm/min at 300 and 125 °C on Si(001) and Ge(001) substrates, respectively. The CoFe layer was deposited from a rod-type CoFe source having a composition of $Co_{70}Fe_{30}$ (in atomic percent) with a deposition rate of 0.25 nm/min at RT. The sample was subsequently annealed *in situ* for 30 min at 300 °C to improve the surface morphology and crystallinity. Finally, the sample was capped by a 2-nm-thick Cr layer at RT to prevent the oxidation of the sample. The structural characterization using *in situ* reflective high-energy electron diffraction (not shown) and *ex situ* transmission electron microscopy [Figs. 1(a) and 1(b)] confirmed the highly (001) textured and single-crystalline structures of CoFe/MgO/Si and CoFe/MgO/Ge samples, respectively, with smooth

 ©2013 American Physical Society

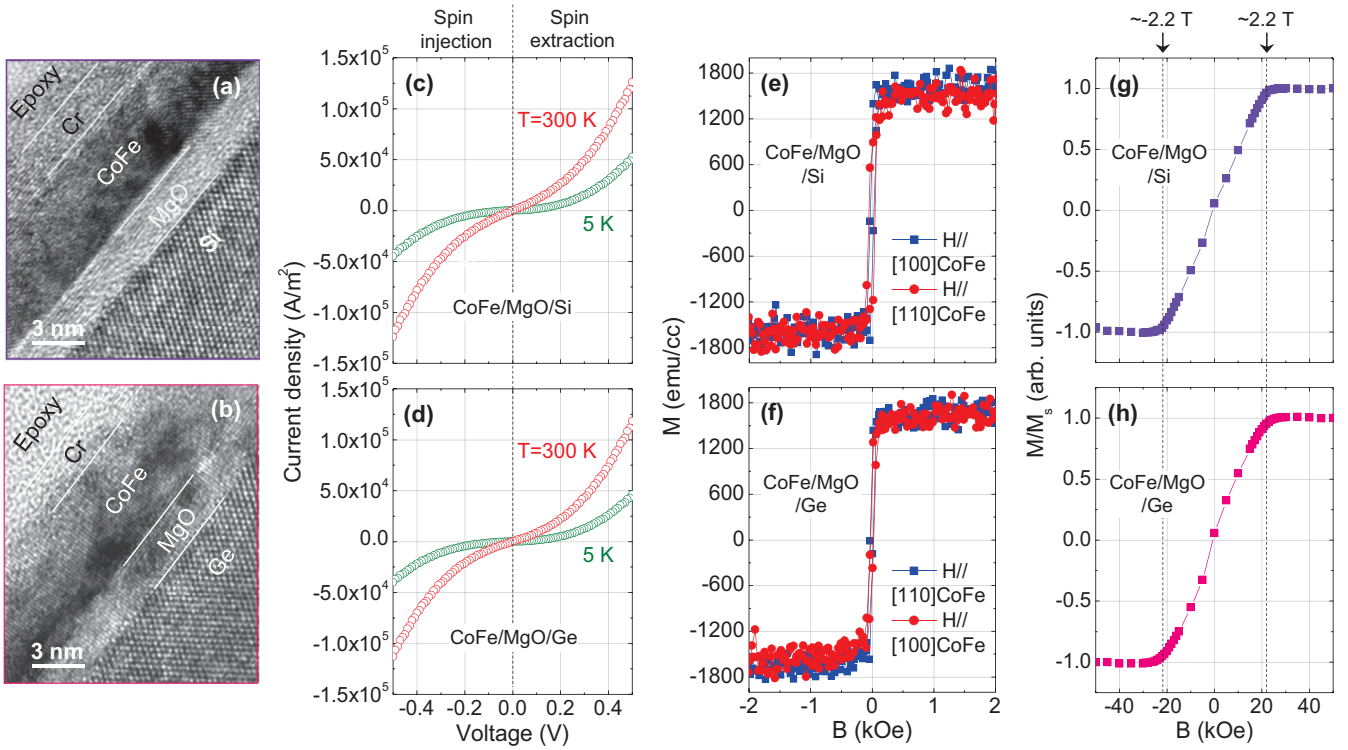

FIG. 1. (Color online) High-resolution tunneling electron microscope (TEM) images of (a) CoFe(5 nm)/MgO(2 nm)/Si(001) and (b) CoFe(5 nm)/MgO(2 nm)/Ge(001) samples. Typical *J*-*V* characteristics of (c) CoFe/MgO/Si and (d) CoFe/MgO/Ge tunnel contacts at 300 and 5 K. Representative *M*-*H* loops of (e) CoFe/MgO/Si and (f) CoFe/MgO/Ge samples along the [110] and [100] directions of CoFe with in-plane fields. *M*-*H* loops of (g) CoFe/MgO/Si and (h) CoFe/MgO/Ge samples with perpendicular fields.

interfaces. To measure the electrical OHE in the ferromagnetic tunnel contacts, we fabricated devices consisting of multiple CoFe/MgO/SC tunnel contacts ($100 \times 100\ \mu m^2$). Details of the sample preparation as well as the structural characterization of the samples are available in the literature.[14]

It should be noted that the dominant transport mechanism for both contacts (CoFe/MgO/Si and CoFe/MgO/Ge) is tunneling, as proven by the symmetric *I*-*V* curve and its weak *T* dependence in Figs. 1(c) and 1(d); both types of contacts exhibit the small resistance-area (RA) products of $\sim 5 \times 10^{-6}\ \Omega\ m^2$ (300 K) to $\sim 1 \times 10^{-5}\ \Omega\ m^2$ (5 K) at the constant bias voltage ($V_{B=0}$) of -0.3 V, which is associated with the narrow depletion region of $\sim$5 nm.

To estimate the magnitude of the local magnetostatic field (B_L^{ms}), which scales with the roughness of the FM interface and the magnetization (M) of the FM,[15,16] we have characterized the roughness of MgO/SC reference samples without CoFe using atomic force microscopy (AFM) and the magnetic property of complete CoFe/MgO/SC samples using a vibrating sample magnetometry (VSM) and a superconducting quantum interference device (SQUID). The MgO/SC reference samples show a root-mean-square (RMS) roughness of $\sim$0.2 nm, peak-to-peak height variations of $\sim$0.3–0.4 nm, and lateral correlation lengths of $\sim$30–50 nm (not shown). The CoFe/MgO/SC samples have saturation magnetization (M_s) values of $\sim 1600 \pm 150$ emu/cm^3 (CoFe/MgO/Si) and $\sim 1650 \pm 150$ emu/cm^3 (CoFe/MgO/Ge) with a normalized remanence (M_r/M_s, where M_r is remanent magnetization) of $\sim$0.93 (CoFe/MgO/Si) and $\sim$0.95 (CoFe/MgO/Ge) for the (in-plane) easy-axis magnetization as shown in Figs. 1(e) and 1(f). Both CoFe/MgO/Si and CoFe/MgO/Ge samples do not have a noticeable magnetic anisotropy in the film plane. The normalized magnetization (M/M_s) values in the CoFe/MgO/SC samples saturate at $\sim$2.2 T with the perpendicular magnetic field as shown in Figs. 1(g) and 1(h), indicating that the perpendicular magnetic anisotropy is also negligible.

Taking into account the similar depletion width, roughness, and magnetization, it is likely that the magnitude of B_L^{ms} at the interface is not fundamentally different in both CoFe/MgO/Si and CoFe/MgO/Ge contacts.

B. Measurement scheme

Figures 2(a)–2(e) illustrate the electrical detection of the OHE in a FM/oxide/SC tunnel contact by means of the three-terminal measurement scheme, where a single ferromagnetic tunnel contact is used for electrical injection as well as for the detection of the spin accumulation in the SC.[14–20] The direction of the spin injection and the spin detection coincides with the direction of the M of the FM [see Figs. 2(d) and 2(e)].

The OHE signal depends on the magnitude and angle of the external magnetic fields. When an external magnetic field (B^{ext}) much smaller than $\mu_0 M_s$ of FM (where μ_0 is the permeability of free space) is applied at an oblique angle θ to the x axis [Fig. 2(a)], the M of FM almost remains in-plane. The electrically injected spins in the SC under reverse bias

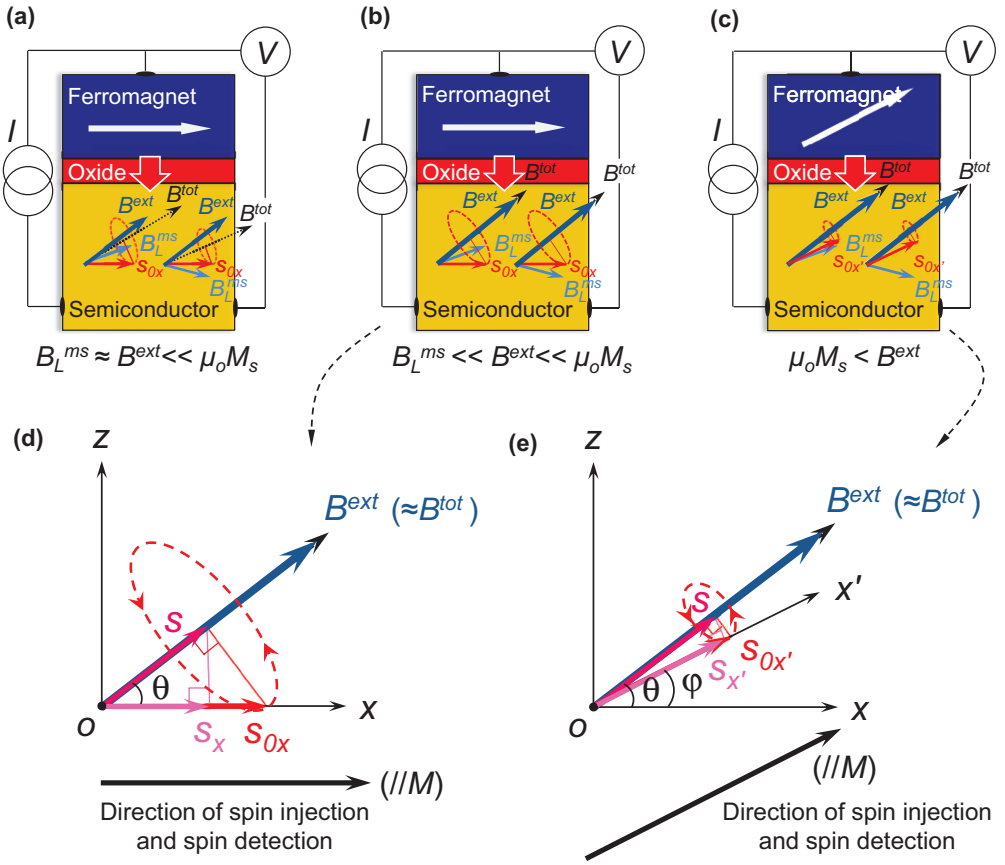

FIG. 2. (Color online) (a)–(e) Schematic illustration of the electrical detection of the oblique Hanle effect (OHE) in a ferromagnet/oxide/semiconductor tunnel contact for different external magnetic field (B^{ext}) ranges using the three-terminal measurement scheme.

($I < 0$) are precessed around the total magnetic field (B^{tot}) direction, given by the vector sum of B_L^{ms} and B^{ext}. It is noteworthy that, even at zero B^{ext}, the injected spins are initially precessed and dephased by B_L^{ms} having random directions at the SC interface.[15,16]

At intermediate values of B^{ext} [$\mu_0 M_s \gg B^{ext} \gg B_L^{ms}$; Fig. 2(b)], the spins are precessed around B^{ext} and the average spins are saturated along the oblique B^{ext}, resulting in an asymptotic value of the spin signal depending on the angle θ [Fig. 2(d)]. The resultant spin signal (S) in SC is reduced to $S_{0x}\cos(\theta)$. Because the same ferromagnetic tunnel contact is used to detect the spin signal, the magnitude of the spin signal (S_x) at the detector is further reduced to $S_{0x}\cos^2(\theta)$.

When a very large B^{ext} exceeding $\mu_0 M_s$ of the FM is applied [Figs. 2(c) and 2(e)], the M of FM is significantly tilted from the film plane to the B^{ext} direction with the tilting angle (φ). The misalignment angle ($\theta - \varphi$) between B^{ext} and M is determined by minimizing the total magnetic energy (E_{tot}) of the FM layer which consists of the Zeeman energy and the demagnetization energy (or shape anisotropy energy),

$$E_{tot} = -M_s B_{ext}\cos(\theta - \phi) + \tfrac{1}{2}\mu_0 M_s^2 \sin^2(\phi), \qquad (1)$$

$$\varphi = \theta - \arctan\left[\mathrm{sgn}(\theta)\sqrt{\left(\frac{\cos(2\theta) + (B_{ext}/\mu_0 M_s)}{\sin(2\theta)}\right)^2 + 1} - \frac{\cos(2\theta) + (B_{ext}/\mu_0 M_s)}{\sin(2\theta)}\right]. \qquad (2)$$

In this case, the misalignment angle ($\theta - \varphi$) can give rise to the OHE, resulting in the angular dependence of the voltage signal proportional to $S_{0x'}\cos^2(\theta - \varphi)$ [Fig. 2(e)].

III. RESULTS AND DISCUSSION

A. Model calculation of the electrical oblique Hanle effect in ferromagnetic tunnel contacts

To obtain insight into the generic features of the electrical OHE (in the ferromagnetic tunnel contact), we calculated the oblique Hanle curves for different spin lifetime values (τ_{sf}) with a fixed value of B_L^{ms} using the spin precession and relaxation model,[16] including the initial spin precession and the dephasing due to the B_L^{ms}. Here we assumed the M of FM is in-plane ($B^{ext} \ll \mu_0 M_s$) for simplicity. The general case, where the M is tilted from the film plane [Fig. 2(c)], will be discussed in Sec. III C.

In the case of electrical spin injection $\vec{S}_i$ (S_{0x},0,0) [see Fig. 2(d)], the S_x component of the steady-state spin polarization $\vec{S}$ at the SC interface, which is parallel to the M direction of the FM detector, in B^{tot} consisting of B_L^{ms} and B^{ext} is expressed as

$$S_x = S_{0x}\left\{\frac{\omega_x^2}{\omega_L^2} + \left(\frac{\omega_y^2 + \omega_z^2}{\omega_L^2}\right)\left(\frac{1}{1 + (\omega_L \tau_{sf})^2}\right)\right\}, \qquad (3)$$

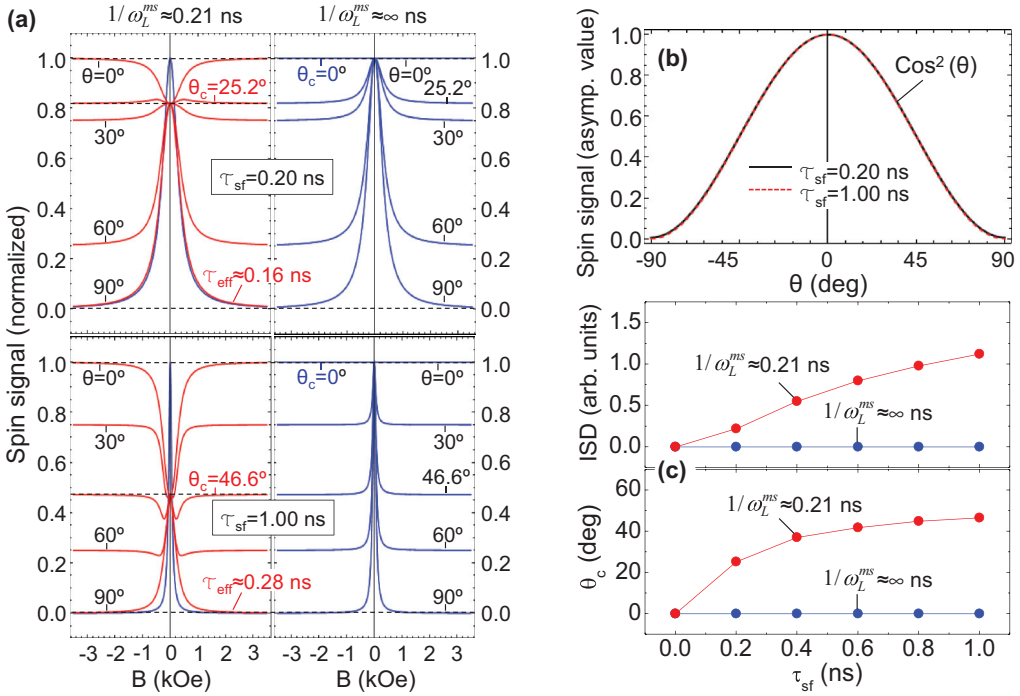

FIG. 3. (Color online) (a) Calculated Hanle curves for various oblique angles (0°–90°) with two different τ_{sf} values of 0.20 and 1.00 ns, respectively, at a fixed $1/\omega_L^{ms}$ value of 0.21 ns. For comparison, the ideal OHE curves, where $B_L^{ms} \approx 0$ kOe (or $1/\omega_L^{ms} \approx \infty$ ns), are also shown (blue lines). (b) Asymptotic values of the OHE vs θ for the two τ_{sf} values of 0.20 and 1.00 ns. (c) Calculated interfacial spin depolarization (ISD) $[S_{0x} - S_x(B^{ext} = 0)/S_x(B^{ext} = 0)]$ and critical oblique angle (θ_c) $-\tau_{sf}$ plots for two different $1/\omega_L^{ms}$ values of 0.21 (red symbol) and ∞ ns (blue symbol).

where S_{0x} is the injected spin polarization without any magnetic field, ω_L $(= g\mu_B B_{tot}/\hbar)$ is the Larmor frequency, $\omega_L^2 = \omega_x^2 + \omega_y^2 + \omega_z^2$, and $\omega_i = \omega_i^{ext} + \omega_i^{ms}(x,y,z)$. Here, g is the Landé $g-$factor, μ_B is the Bohr magneton, $\hbar$ is the Planck constant divided by 2π, and $\omega_i^{ms}(x,y,z)$ was set such that it had periodic spatial variation with $\omega_L^{ms}\cos(2\pi x/\lambda)$, where $\omega_L^{ms} \approx 4.7$ ns^{-1} (or $1/\omega_L^{ms} \approx 0.21$ ns, corresponding to a B_L^{ms} value of 0.3 kOe) and $\lambda = 40$ nm and where the spin polarization was averaged in space over a full period λ for simplicity.

Two important features of the electrical OHE are obtained from the calculated Hanle curves [normalized, Fig. 3(a)] at various angles (0°–90°) with two different spin lifetimes (τ_{sf}) of 0.20 and 1.00 ns, respectively, at a fixed $1/\omega_L^{ms}$ value of 0.21 ns. For comparison, ideal OHE curves, where $B_L^{ms} \approx 0$ kOe (or $1/\omega_L^{ms} \approx \infty$ ns), are also shown [blue lines; right panels of Fig. 3(a)]. The first feature shows that the oblique Hanle line shapes are significantly dependent on τ_{sf} (at a fixed value of $1/\omega_L^{ms}$). For a large value of τ_{sf}, the inverted OHE, indicative of the initial spin suppression due to B_L^{ms},[15,16] becomes pronounced as the θ value approaches 0°; the width of the oblique Hanle curve at the angle θ of 90° (red line) is remarkably broadened in comparison with the ideal Hanle curve (blue line) without B_L^{ms}. The injected spins with a large value of τ_{sf} (strictly, $\tau_{sf} \geqslant 1/\omega_L^{ms}$) are precessed many times in B_L^{ms} and randomized within their values of τ_{sf}. This results in the sizable suppression of the spin polarization and spin coherence, as discussed in the literature.[15]

The second feature is that, in spite of the different features of the electrical OHE (depending on the values of τ_{sf} and $1/\omega_L^{ms}$), their asymptotic values at a high B^{ext} are identical [see the top and bottom panels of Fig. 3(a)]. For a more quantitative analysis, we plotted the asymptotic value of the OHE versus θ for the two τ_{sf} values of 0.20 and 1.00 ns. As shown in Fig. 3(b), the asymptotic value of the electrical OHE depends only on the angle θ, thus revealing the unique dependence on $\cos^2(\theta)$. This result is predicted by Eq. (3). When $B^{ext} \gg B_L^{ms}$ (or $B^{ext} \approx B^{tot}$) and $\omega_L\tau_{sf} \gg 1$, the normalized S_x value is determined only by the ratio of the B^{ext} component, $(B_x^{ext})^2/(B^{ext})^2$, which can be written in terms of the angle θ, $\cos^2(\theta)$.

In addition, from the electrical OHE measurements, it is possible to extract the critical oblique angle (θ_c): the smallest angle θ at which the asymptotic value of the OHE signal coincides with the Hanle signal at zero B^{ext} [see Fig. 3(a)], $\theta_c \equiv \arccos[\sqrt{S_x(B^{ext} = 0)/S_{0x}}]$. This can be another quantitative measure of the effect of B_L^{ms} on the spin accumulation in SC. In Ref. 15, we have introduced a physical quantity called the interfacial spin depolarization (ISD), defined as $[S_{0x} - S_x(B^{ext} = 0)]/S_x(B^{ext} = 0)$. This quantity describes how much the spin accumulation in SC has been decreased due to the initial spin precession and dephasing caused by B_L^{ms}.[15,16] The θ_c value is determined by τ_{sf} and B_L^{ms}. If $\tau_{sf} \ll 1/\omega_L^{ms}$($B_L^{ms}$ is small), the spins are completely relaxed within their spin lifetime before being precessed by B_L^{ms}. In this case, the suppression of spin accumulation by B_L^{ms} is negligible, leading to a small θ_c. In contrast, if $\tau_{sf} \geqslant 1/\omega_L^{ms}$($B_L^{ms}$ is large), the θ_c becomes pronounced because the spins are precessed many times in B_L^{ms} and randomized within their τ_{sf}, resulting in the sizable suppression of the spin polarization by B_L^{ms}. Figure 3(c)

shows the calculated ISD and $\theta_c - \tau_{sf}$ plots for two different $1/\omega_L^{ms}$ values of 0.21 and ∞ ns. When $1/\omega_L^{ms} \approx \infty$ ns (or $B_L^{ms} \approx 0$ kOe; blue symbol), the ISD and corresponding θ_c are negligible irrespective of τ_{sf}.[15] In contrast, when $1/\omega_L^{ms} \approx 0.21$ ns (or $B_L^{ms} \approx 0.3$ kOe; red symbol), the ISD and corresponding θ_c are strongly enhanced as a function of τ_{sf}.[15]

B. Experimental observation of the electrical oblique Hanle signals in CoFe/MgO/Si and CoFe/MgO/Ge contacts

We experimentally checked whether the electrical OHEs obtained in the CoFe/MgO/Si and CoFe/MgO/Ge contacts show the features consistent with the above model calculations. At the beginning of each Hanle measurement, we applied a large enough in-plane magnetic field (>1 T) along the easy magnetization axis to create homogeneous in-plane magnetization in each contact, and thereafter we decreased the in-plane magnetic field to zero. A constant bias current (I) is applied across the tunnel contact while the V is measured as a function of applied B^{ext} at a fixed angle θ [see Figs. 2(a) and 2(b)]. It is noteworthy that the control experiments[4,5,17] using a nonmagnetic interfacial layer confirm that the observed Hanle signals in our system are genuine and arise from the spin accumulation.

Figures 4(a) and 4(b) show the obtained OHE signals ($|\Delta V_{OHE}|$) at various θ in the CoFe/MgO/Si and CoFe/MgO/Ge contacts, respectively, applying I of -0.5 mA (spin injection condition) at 300 and 5 K. At RT [the top panels of Figs. 4(a) and 4(b)], the CoFe/MgO/Si contact with an effective value of τ_{sf} (τ_{eff}) of 106 ps, as extracted from the Lorentzian fit of the Hanle curve at an angle θ of 90° (note that

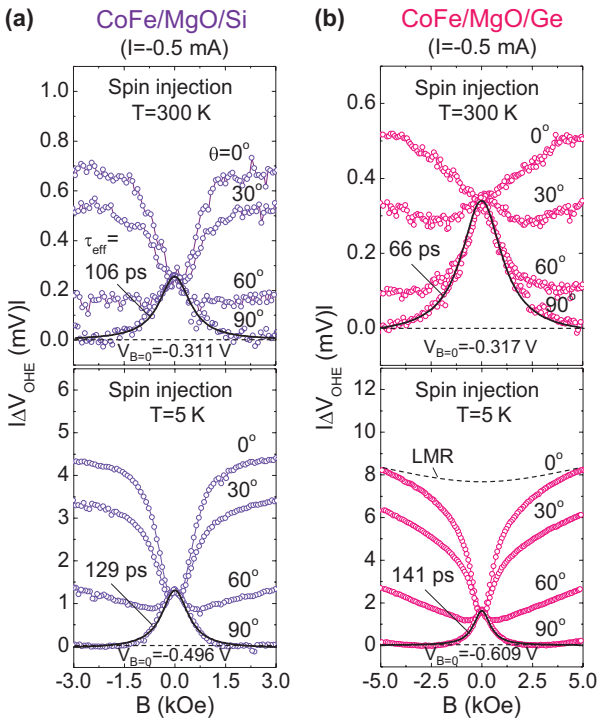

FIG. 4. (Color online) Obtained OHE signals ($|\Delta V_{OHE}|$) in the (a) CoFe/MgO/Si and (b) CoFe/MgO/Ge contacts, respectively, at the bias current (I) of -0.5 mA (spin injection condition) with various θ values for 300 and 5 K.

the extracted τ_{eff} value should be considered as the lower bound for the τ_{sf} due to the artificial broadening of the Hanle curve caused by the B_L^{ms}),[15,16] shows a pronounced inverted Hanle signal at θ of 0° and 30°. In contrast, the inverted Hanle effect is relatively weak for the CoFe/MgO/Ge contact having a τ_{eff} value of 66 ps. At a low T of 5 K [bottom panels of Figs. 4(a) and 4(b)], the τ_{eff} values increase and the inverted OHEs at the θ values of 0° and 30° become larger; moreover, the increases of τ_{eff} and the inverted OHEs of the CoFe/MgO/Ge contact are more pronounced than those of the CoFe/MgO/Si contact, both of which are consistent with the findings in previous work.[15] Considering that the magnitude of the B_L^{ms} (at the SC interface) and the related T dependence are not fundamentally different in both contacts, it is clear that the different features of the electrical OHE in the CoFe/MgO/Si and CoFe/MgO/Ge contacts are mainly ascribed to the different τ_{sf} values,[15] as predicted by the model calculation.

It should be mentioned here that the obtained spin-RA values of 14 (88) kΩ μm^2 for CoFe/MgO/Si and 10 (164) kΩ μm^2 for CoFe/MgO/Ge at I of -0.5 mA (spin injection condition) at 300 (5) K are several orders of magnitude larger than the expected values from the existing spin injection and diffusion theory.[21] This discrepancy between experiment and theory in the three-terminal Hanle measurement has been consistently observed with many types of tunnel barrier and SC, as discussed in the Ref. 4. The origins of this discrepancy, i.e., other enhancement factors not yet incorporated in the existing theory, are still under investigation.[5]

Another important feature of the electrical OHE is the unique angular dependence of the asymptotic value of the oblique Hanle signal. In the model calculation [see Fig. 3(b)], it is expected that the asymptotic value at an intermediate value of B^{ext} [$\mu_0 M_s \gg B^{ext} \gg B_L^{ms}$ (or $B^{ext} \approx B^{tot}$) and $\omega_L \tau_{sf} \gg 1$] shows the $\cos^2(\theta)$ dependence on the angle θ. To check this, we measured the asymptotic values of $|\Delta V_{OHE}|$ of the CoFe/MgO/Si and CoFe/MgO/Ge contacts as a function of the angle θ with oblique B^{ext} values of 3 and 5 kOe, respectively.

An oblique B^{ext} applied under the angle θ in the direction of the (in-plane) easy axis M of the FM [x axis, see Figs. 2(d) and 2(e)] will force M to be tilted out of plane by the amount of the tilting angle (φ). Using Eq. (2), we calculated the tilting angle φ as a function of the field angle θ when the B^{ext} is 3 kOe (CoFe/MgO/Si) and 5 kOe (CoFe/MgO/Ge) and the $\mu_0 M_s$ of CoFe is 2.2 T [see Figs. 1(g) and 1(h)]. As depicted in Fig. 5(a), the $\varphi(\theta)$ values do not exceed 9° for CoFe/MgO/Si and 14° for CoFe/MgO/Ge contacts. If we measure the $|\Delta V(\theta)|$ as a function of angle θ (from in-plane to out-of-plane), the measured voltage is proportional to $S_{0x'} \cos^2(\theta - \varphi)$ as explained in Sec. III A. As a consequence, we can obtain different curves depending on the magnitude of B^{ext}. Figure 5(b) shows the calculated $\Delta V_{OHE,\ asym.\ value}(\theta)$ curves for three different cases: (i) $\varphi(\theta) = 0$ (black dashed line) when B^{ext} is small enough to retain in-plane M, (ii) $\varphi(\theta) \neq 0$ when $B^{ext} = 3$ kOe (purple line), and (iii) $\varphi(\theta) \neq 0$ when $B^{ext} = 5$ kOe (pink line). In this calculation, we assumed that the tunnel spin polarization and spin lifetime do not have a significant angular dependence ($S_{0x'} \approx S_{0x}$) because of the low tilting angles. We have noticed that the $\Delta V_{OHE,\ asym.\ value}(\theta)$ curves deviate slightly from the ideal case [no tilting; $\varphi(\theta) = 0$; black dashed line]. From this, we can

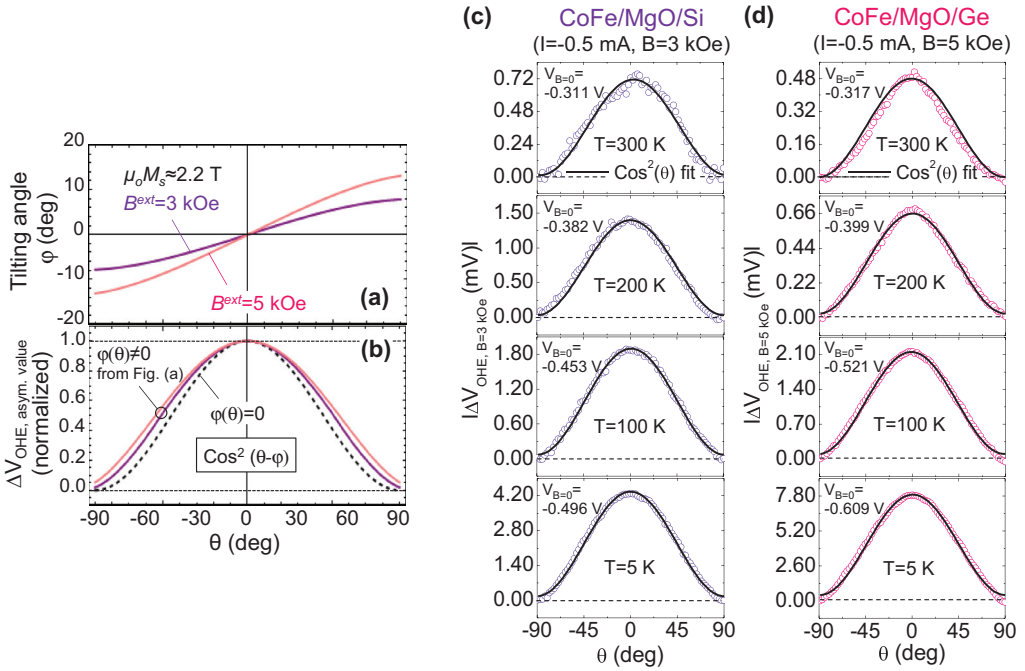

FIG. 5. (Color online) (a) The tilting angle (φ) variation with θ at the B^{ext} values of 3 (for CoFe/MgO/Si) and 5 kOe (for CoFe/MgO/Ge). (b) Calculated $\Delta V_{\text{OHE, asym. value}}(\theta)$ curves for the B^{ext} values of 3 (for CoFe/MgO/Si) and 5 kOe (for CoFe/MgO/Ge) using the $\varphi(\theta)$ values exhibited in Fig. 5(a). For comparison, the ideal $\Delta V_{\text{OHE, asym. value}}$ (θ) curve, where there is no tilting ($\varphi = 0$), is also shown (black dashed line). Asymptotic value of $|\Delta V_{\text{OHE}}|$ (or $|\Delta V_{\text{OHE, } B=3 \text{ or } 5 \text{ kOe}}|$) vs θ obtained in (c) CoFe/MgO/Si and (d) CoFe/MgO/Ge contacts at the I value of -0.5 mA (spin injection condition) at different temperatures.

conclude that the tilting of M with a B^{ext} smaller than 5 kOe does not significantly affect the major angular dependence of the OHE signal proportional to $\cos^2(\theta)$.

Figures 5(c) and 5(d) show the asymptotic value of $|\Delta V_{\text{OHE}}|$ (or $|\Delta V_{\text{OHE, } B=3 \text{ or } 5 \text{ kOe}}|$) versus θ measured with the CoFe/MgO/Si and CoFe/MgO/Ge contacts, respectively, at the I of -0.5 mA (spin injection condition) at different temperatures. These figures clearly show that the asymptotic values of the oblique Hanle signals in both contacts are consistently reduced by a factor of $\cos^2(\theta)$ (black lines) over a wide T range (5–300 K). This result is in good agreement with the model prediction, in which the asymptotic value of the electrical OHE depends only on the angle θ, revealing the unique $\cos^2(\theta)$ dependence.

As discussed in Sec. III A, from the electrical OHE measurements, we can extract the critical angle θ_c ($\theta_c \equiv \arccos[\sqrt{S_x(B_{\text{ext}} = 0)/S_{0x}}]$) which is the quantitative measure (with angular dimension) of the ISD. Figure 6 shows the temperature dependence of θ_c, ISD ($\equiv[S_{0x} - S_x(B^{\text{ext}} = 0)]/S_x(B^{\text{ext}} = 0)$), and τ_{eff} measured with the CoFe/MgO/Si and CoFe/MgO/Ge contacts. A large θ_c(or a large ISD) indicates that the spin signal is sizably suppressed by B_L^{ms}. We have indeed observed the large θ_c value of 52° (36°) for the CoFe/MgO/Si (CoFe/MgO/Ge) contact at 300 K. As T is decreased from 300 to 5 K, the θ_c is increased from 52° (300 K) to 58° (5 K) for the CoFe/MgO/Si contact, and from 36° (300 K) to 66° (5 K) for the CoFe/MgO/Ge contact. As discussed in Sec. III A, the θ_c is related to both τ_{sf} and B_L^{ms}. Because $B_L^{\text{ms}}(T) \propto (1 - \alpha T^{3/2})$ with $\alpha = 3.2 \times 10^{-5}$ K$^{-3/2}$ for the CoFe,[22,23] the T dependence of ω_L^{ms} is relatively weak. Therefore, the increase of θ_c with decreasing T in both contacts is mainly ascribed to the increased τ_{sf} [see Fig. 3(c)]. This result is consistent with the observation that the measured τ_{eff} (a lower bound of true spin

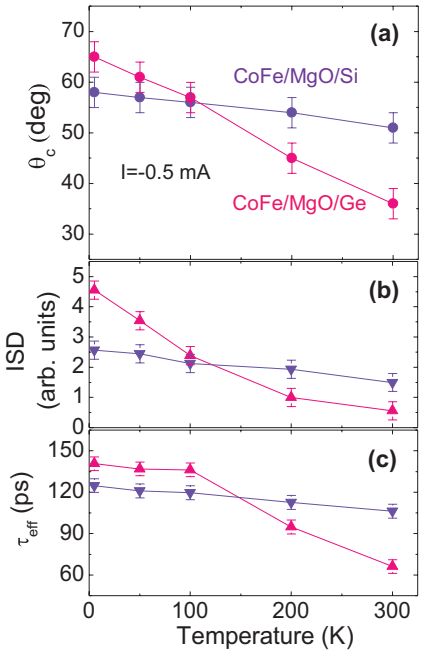

FIG. 6. (Color online) (a) Measured θ_c, (b) ISD ($|\Delta V_{\theta=0^\circ}/\Delta V_{\theta=90^\circ}|$), and (c) effective spin lifetime (τ_{eff}) in the CoFe/MgO/Si and CoFe/MgO/Ge contacts as a function of the temperature (T) at the I value of -0.5 mA.

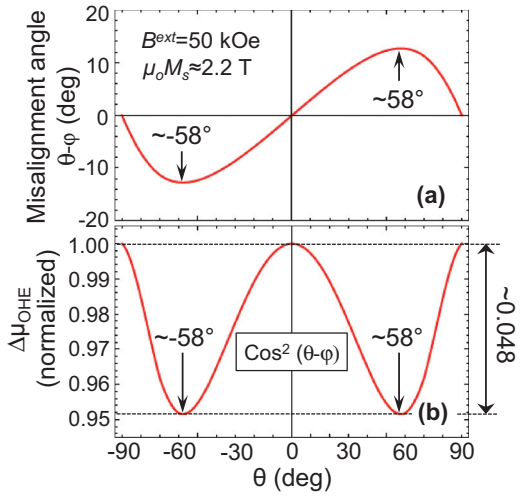

FIG. 7. (Color online) (a) Calculated misalignment angle $(\theta - \varphi)$ and (b) corresponding $\Delta\mu_{\mathrm{OHE}}$ (normalized) as a function of B^{ext} angle θ at the B^{ext} and $\mu_0 M_s$ values of 50 kOe and ~2.2 T, respectively.

lifetime in SC) is increased with decreasing T as shown in Fig. 6(c).

C. Angular dependence of voltage signals at large magnetic fields

Next we investigated the angular dependence of voltage $[|\Delta V(\theta)|]$ signals when the applied B^{ext} is larger than $\mu_0 M_s$. In this case, as discussed previously, the M is significantly tilted from the film plane to the B^{ext} direction [see Figs. 2(c) and 2(e)]. When we measure the spin accumulation $(\Delta\mu_{\mathrm{OHE}})$ as a function of angle θ (from in-plane to out-of-plane), the $\Delta\mu_{\mathrm{OHE}}(\theta)$ does not follow a simple $\cos^2(\theta)$ angular dependence.

If the M perfectly followed the applied B^{ext} (when $B^{\mathrm{ext}} = \infty$), there would be no angular dependence of $\Delta\mu_{\mathrm{OHE}}$ arising from the OHE.[24] However, the misalignment angle $(\theta - \varphi)$ between the applied B^{ext} and the M of the CoFe is non-negligible even when B^{ext} is very large [see Eq. (2)]. Figure 7(a) shows the calculated angle $(\theta - \varphi)$ as a function of angle θ when the B^{ext} is 50 kOe and the $\mu_0 M_s$ of CoFe is 2.2 T. The misalignment angle $(\theta - \varphi)$ is smaller than 12° having extrema at $-58°$ and 58°. If the tunnel spin polarization and spin lifetime do not have a significant angular dependence $(S_{0x'} \approx S_{0x})$,[24] the spin accumulation $[\Delta\mu_{\mathrm{OHE}}(\theta)]$ is proportional to $S_{0x}\cos^2(\theta - \varphi)$. Therefore, the $\Delta\mu_{\mathrm{OHE}}(\theta)$ does not follow a simple $\cos^2(\theta)$ angular dependence, but follows a more complex $\cos^2(\theta - \varphi)$ angular dependence as depicted in Fig. 7(b). The variation of $\Delta\mu_{\mathrm{OHE}}$ (normalized) as a function of θ with large magnetic fields is relatively smaller than the case with small magnetic fields. For example, in Fig. 7(b), the variation of $\Delta\mu_{\mathrm{OHE}}$ (at the B^{ext} of 50 kOe) is less than 5% of full spin accumulation.

We have indeed measured the $|\Delta V(\theta)|$ of the CoFe/MgO/Si and CoFe/MgO/Ge contacts with moderate magnetic fields (3 or 5 kOe) and with a large magnetic field (50 kOe) at various reverse bias currents ($I < 0$; spin injection condition) at 5 K. Figures 8(a) and 8(b), respectively, are obtained with applying the B^{ext} of 3 kOe for the CoFe/MgO/Si contact and 5 kOe for the CoFe/MgO/Ge contact. The $|\Delta V_{B=3 \text{ or } 5\ \mathrm{kOe}}|$ signals in both contacts clearly reveal a $\cos^2(\theta)$ dependence (black lines) irrespective of I, which is well consistent with the generic feature of the OHE; both contacts exhibit the twofold symmetry with the peak at an angle θ of 0° as well as valleys at θ angles of $-90°$ and 90°. The magnitudes of the MR values, defined as $(\Delta V / V_{\theta=90°}|_{B=3 \text{ or } 5\ \mathrm{kOe}}) \times 100\%$, are ~1.0 (CoFe/MgO/Si) and ~1.2% (CoFe/MgO/Ge) at 5 K.

Figures 8(c) and 8(d), respectively, are obtained by applying the large B^{ext} of 50 kOe for the CoFe/MgO/Si and

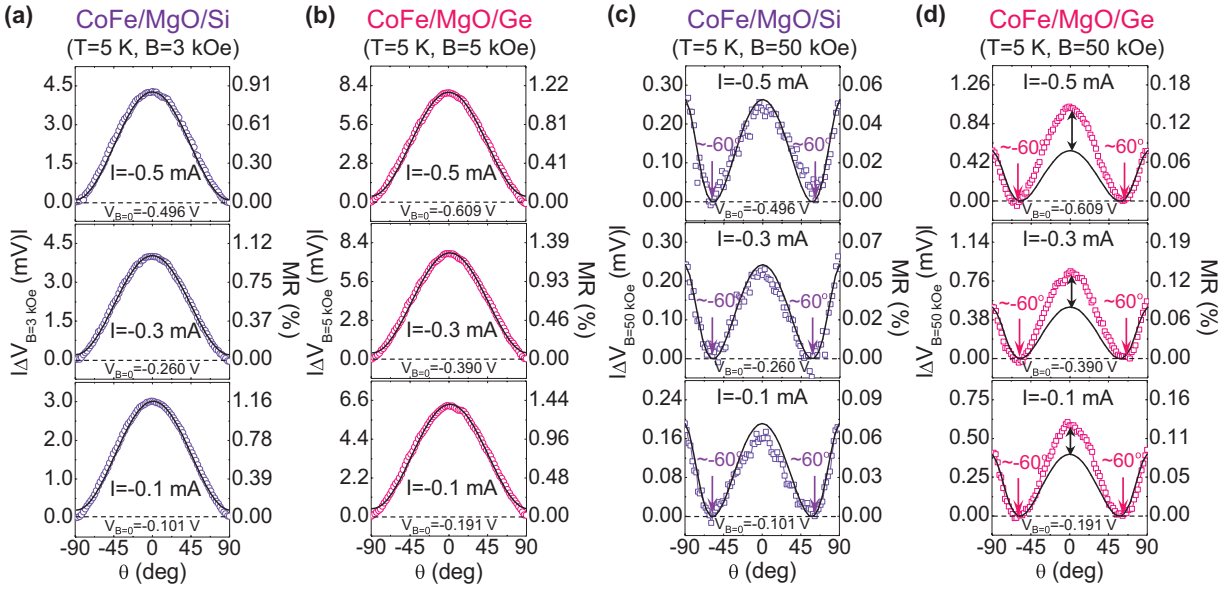

FIG. 8. (Color online) (a), (b) $|\Delta V_{B=3 \text{ or } 5\ \mathrm{kOe}}|$ and (c), (d) $|\Delta V_{B=50\ \mathrm{kOe}}|$ signals vs θ curves for the CoFe/MgO/Si contact [(a), (c)] and the CoFe/MgO/Ge contact [(b), (d)] with various reverse bias current ($I < 0$; spin injection condition) at 5 K. Black lines in (a) and (b) are $\cos^2(\theta)$ fits. Black lines in (c) and (d) are $\cos^2(\theta - \varphi)$ fits.

CoFe/MgO/Ge contacts. Basically, the $|\Delta V_{B=50\ \mathrm{kOe}}|$ signals of both contacts show distorted fourfold symmetry with valleys at θ angles of -60° and 60° and peaks at θ angles of -90°, 0°, and 90°. The MR values, defined as $(\Delta V/V_{\theta=60^\circ}|_{B=50\ \mathrm{kOe}}) \times 100\%$, of ~0.05 (CoFe/MgO/Si) and ~0.10% (CoFe/MgO/Ge) at 5 K are roughly one order of magnitude smaller than the MR measured at moderate magnetic fields (3 or 5 kOe). The $\cos^2(\theta-\varphi)$ dependence [black lines in Fig. 8(c)] provide a reasonably good fit to the experimental data of $|\Delta V_{B=50\ \mathrm{kOe}}|$ in the CoFe/MgO/Si contact, indicating that the angular dependence of voltage signals with large magnetic fields is a consequence of the misalignment between the B^{ext} and the M of CoFe [see Fig. 2(e)]. The CoFe/MgO/Ge data deviate from the $\cos^2(\theta-\varphi)$ fit when the θ value is close to 0° [black arrows in Fig. 6(d)]. This may be attributed to the Lorentz MR (LMR)[24] of the Ge substrate with a relatively high mobility, since the LMR, originated from the influence of the Lorentz force on the motion of electrons, is quadratically proportional to the mobility times the transverse B to the current flow.[25]

We have measured the bias dependence of the full spin accumulation $|\Delta V_{\mathrm{spin}}|$ and the variation of $|\Delta V_{\mathrm{OHE},\ B=50\ \mathrm{kOe}}|$ with respect to the angle θ, and we calculated the ratio $|\Delta V_{\mathrm{OHE},\ B=50\ \mathrm{kOe}}/\Delta V_{\mathrm{spin}}|$. The $|\Delta V_{\mathrm{spin}}|$ is the sum of the normal and inverted Hanle signal, and thus can be determined from $|\Delta V_{\theta=0^\circ} - \Delta V_{\theta=90^\circ}|_{B=3\ \mathrm{or}\ 5\ \mathrm{kOe}}$[see Figs. 8(a) and 8(b)]. The $|\Delta V_{\mathrm{OHE},B=50\ \mathrm{kOe}}|$ can be determined from $|\Delta V_{\theta=90^\circ} - \Delta V_{\theta=60^\circ}|_{B=50\ \mathrm{kOe}}$ [see Figs. 8(c) and 8(d)]. The ratio of $|\Delta V_{\mathrm{OHE},\ B=50\ \mathrm{kOe}}/\Delta V_{\mathrm{spin}}|$ will show how much the spin signal is reduced due to the misalignment between the applied B^{ext} and the M of CoFe.

Figure 9 shows the $|\Delta V_{\mathrm{spin}}|$, $|\Delta V_{\mathrm{OHE},\ B=50\ \mathrm{kOe}}|$, and $|\Delta V_{\mathrm{OHE},\ B=50\ \mathrm{kOe}}/\Delta V_{\mathrm{spin}}|$ of the CoFe/MgO/Si and CoFe/MgO/Ge contacts with various reverse bias currents ($I<0$; spin injection condition) at 5 K. Both the $|\Delta V_{\mathrm{spin}}|$ and $|\Delta V_{\mathrm{OHE},\ B=50\ \mathrm{kOe}}|$ increase with increasing the bias current in the same way. In Fig. 9(c), one can clearly see that the $|\Delta V_{\mathrm{OHE},\ B=50\ \mathrm{kOe}}/\Delta V_{\mathrm{spin}}|$, the ratio of reduced spin signal due to the misalignment-induced OHE, remains almost constant with varying the I. The measured $|\Delta V_{\mathrm{OHE},\ B=50\ \mathrm{kOe}}/\Delta V_{\mathrm{spin}}|$ is ~0.060 (0.065) for the CoFe/MgO/Si (CoFe/MgO/Ge) contact. This is very close to the calculated value of ~0.048 (black circles) in Fig. 7. These results strongly support the idea that the observed $|\Delta V(\theta)|$ signals at high magnetic fields in CoFe/MgO/Si and CoFe/MgO/Ge contacts (under spin injection condition) mainly originate from the variation of $\Delta\mu_{\mathrm{OHE}}$ due to the misalignment between the applied B^{ext} and the M of CoFe.

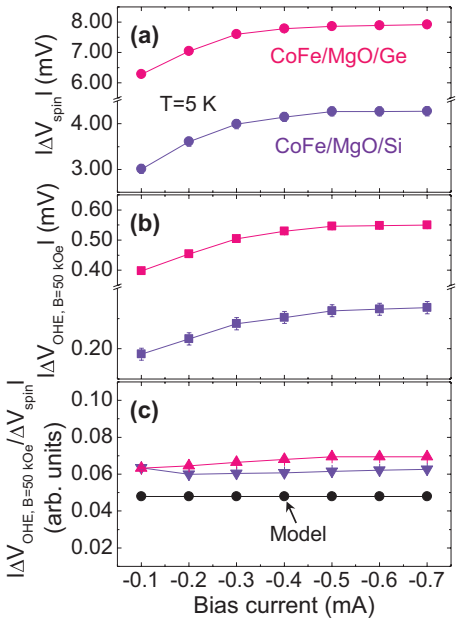

FIG. 9. (Color online) (a) Measured $|\Delta V_{\mathrm{spin}}|$, (b) $|\Delta V_{\mathrm{OHE},\ B=50\ \mathrm{kOe}}|$, and (c) $|\Delta V_{\mathrm{OHE},\ B=50\ \mathrm{kOe}}/\Delta V_{\mathrm{spin}}|$ values for the CoFe/MgO/Si and CoFe/MgO/Ge contacts with various reverse bias currents ($I<0$; spin injection condition) at 5 K. The black circles represent the expected value from the model calculation.

IV. CONCLUSIONS

In conclusion, we investigated the electrical OHE in CoFe/MgO/Si and CoFe/MgO/Ge contacts and their generic features using a three-terminal measurement scheme. The electrical OHE signals obtained in the CoFe/MgO/Si and CoFe/MgO/Ge contacts show clearly different line shapes depending on the spin lifetime of the host SC. Importantly, irrespective of the bias current and temperature, the asymptotic values of the OHE in both contacts reveal the universal angular dependence with $\cos^2(\theta)$ variation with moderate magnetic fields. These results are highly consistent with the predictions of the spin precession and relaxation model for the electrical OHE. The angular dependence of voltage signals observed at high magnetic fields where the magnetization of CoFe is significantly tilted from the film plane to the magnetic field direction is also well explained by the OHE, taking into account the misalignment angle between the external magnetic field and the magnetization of CoFe.

ACKNOWLEDGMENTS

This work was supported by the DGIST R&D Program of the Ministry of Education, Science and Technology of Korea (11-IT-01); by the KIST institutional program (2E22732 and 2V02720) and by the Pioneer Research Center Program (2011-0027905); and by the KBSI Grant No. T33517 for S.-Y.P. The authors would like to thank H. Saito and R. Jansen at AIST for the magnetic characterization by SQUID and for helpful discussions.

APPENDIX: EFFECT OF LOCAL MAGNETOSTATIC FIELD STRENGTH ON OBLIQUE HANLE CURVES

We have investigated the effect of a local magnetostatic field (B_L^{ms}) on the line shapes of oblique Hanle signals obtained in CoFe/MgO/Si and CoFe/MgO/Ge contacts for completeness. The electrical oblique Hanle curves are calculated for different $1/\omega_L^{\mathrm{ms}}$ values of 0.06, 0.21, and 0.64 ns (corresponding to B_L^{ms} values of about 1.0, 0.3, and 0.1 kOe, respectively) with fixed τ_{sf} values of 0.50 and 1.00 ns, using the spin precession and relaxation model[16] [Eq. (3)].

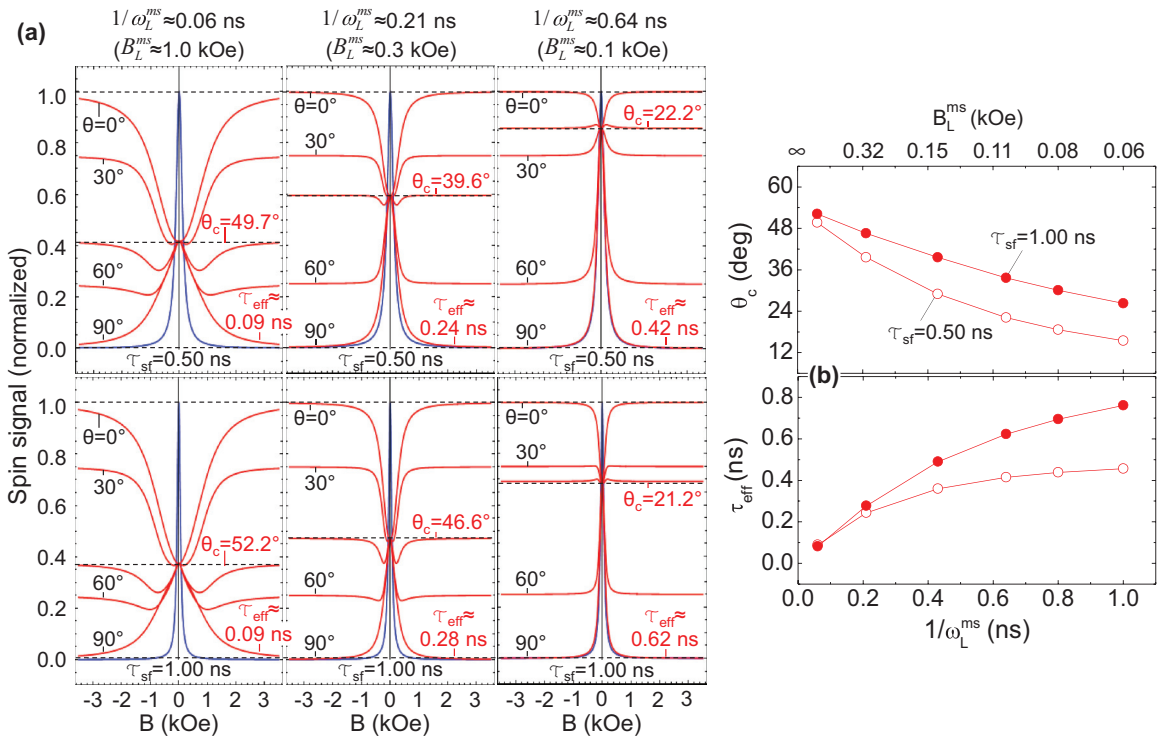

FIG. 10. (Color online) (a) Calculated Hanle curves for various oblique angles (0°–90°) with different $1/\omega_L^{ms}$ values of 0.06, 0.21, and 0.64 ns, at the fixed τ_{sf} values of 0.50 (upper panel) and 1.00 ns (lower panel). For comparison, the ideal Hanle curve, where $B_L^{ms} \approx 0$ kOe (or $1/\omega_L^{ms} \approx \infty$ ns), at the angle θ of 90°, is also shown (blue line). (b) Calculated θ_c and $\tau_{eff} - 1/\omega_L^{ms}$ plots with the fixed τ_{sf} values of 0.50 (open circle) and 1.00 ns (closed circle).

Figure 10(a) shows the calculated oblique Hanle curves (normalized) at various angles (0°–90°). For comparison, the ideal oblique Hanle curve at the angle θ of 90°, where $B_L^{ms} \approx 0$ kOe (or $1/\omega_L^{ms} \approx \infty$ ns), is also shown (blue line). As $1/\omega_L^{ms}$ increases (or B_L^{ms} decreases) with the fixed τ_{sf} value of 0.50 ns (upper panel) or 1.00 ns (lower panel), the inverted Hanle effect becomes smaller; the θ_c also decreases, and the width of the oblique Hanle curve at the angle θ of 90° (red line) approaches that of the ideal Hanle curve (blue line) without B_L^{ms}. Therefore, the effective spin lifetime extracted from the Hanle curve at 90° becomes larger. It should be noticed here that the value of θ_c is inversely correlated with the τ_{eff} value.

For more clarity, we plotted the calculated θ_c and τ_{eff} as a function of $1/\omega_L^{ms}$ with the fixed τ_{sf} values of 0.50 (open circle) and 1.00 ns (closed circle) in Fig. 10(b). As depicted in this figure, the increase of the $1/\omega_L^{ms}$ value (or the decrease of the B_L^{ms} value) results in a decrease of θ_c but an increase of τ_{eff}, which is apparently in contrast with our experimental finding in both CoFe/MgO/Si and CoFe/MgO/Ge contacts that the θ_c is positively correlated with the τ_{eff} (see Fig. 6). As a consequence, we can rule out the possibility that the different Hanle signals observed in CoFe/MgO/Si and CoFe/MgO/Ge contacts originate from the different values of B_L^{ms}.

*scshin@kaist.ac.kr; scshin@dgist.ac.kr

[1] A. Fert, Rev. Mod. Phys. **80**, 1517 (2008).
[2] I. Žutić, J. Fabian, and S. Das Sarma, Rev. Mod. Phys. **76**, 323 (2004).
[3] S. A. Wolf, D. D. Awschalom, R. A. Buhrman, J. M. Daughton, S. von Molnár, M. L. Roukes, A. Y. Chtchelkanova, and D. M. Treger, Science **294**, 1488 (2001).
[4] R. Jansen, Nat. Mater. **11**, 400 (2012).
[5] R. Jansen, S. P. Dash, S. Sharma, and B. C. Min, Semicond. Sci. Technol. **27**, 083001 (2012).
[6] M. Johnson and R. H. Silsbee, Phys. Rev. Lett. **55**, 1790 (1985).
[7] M. Johnson and S. H. Silsbee, Phys. Rev. B **37**, 5326 (1988).
[8] M. I. D'yakonov, V. I. Perel', V. L. Berkovits, and V. I. Safarov, JETP Lett. **40**, 950 (1975).
[9] F. Meier and B. P. Zakharchenya, *Optical Orientation* (North-Holland, Amsterdam, 1984).
[10] V. F. Motsnyi, P. Van Dorpe, W. Van Roy, E. Goovaerts, V. I. Safarov, G. Borghs, and J. De Boeck, Phys. Rev. B **68**, 245319 (2003).
[11] V. F. Motsnyi, V. I. Safarov, J. De Boeck, J. Das, W. Van Roy, E. Goovaerts, and G. Borghs, Appl. Phys. Lett. **81**, 265 (2002).
[12] J. Li, B. Huang, and I. Appelbaum, Appl. Phys. Lett. **92**, 142507 (2008).
[13] C. Awo-Affouda, O. M. J. van 't Erve, G. Kioseoglou, A. T. Hanbicki, M. Holub, C. H. Li, and B. T. Jonker, Appl. Phys. Lett. **94**, 102511 (2009).
[14] K. R. Jeon, C. Y. Park, and S. C. Shin, Cryst. Growth Des. **10**, 1346 (2010); K. R. Jeon, B. C. Min, I. J. Shin, C. Y. Park, H. S. Lee, Y. H. Jo, and S. C. Shin, Appl. Phys. Lett. **98**, 262102 (2011).

[15]K. R. Jeon, B. C. Min, Y. H. Park, Y. H. Jo, S. Y. Park, C. Y. Park, and S. C. Shin, Appl. Phys. Lett. **101**, 022401 (2012).
[16]S. P. Dash, S. Sharma, J. C. LeBreton, J. Peiro, H. Jaffrès, J. M. George, A. Lemaitre, and R. Jansen, Phys. Rev. B **84**, 054410 (2011).
[17]K. R. Jeon, B. C. Min, Y. H. Jo, H. S. Lee, I. J. Shin, C. Y. Park, S. Y. Park, and S. C. Shin, Phys. Rev. B **84**, 165315 (2011).
[18]X. Lou, C. Adelmann, M. Furis, S. A. Crooker, C. J. Palmstrøm, and P. A. Crowell, Phys. Rev. Lett. **96**, 176603 (2006).
[19]S. P. Dash, S. Sharma, R. S. Patel, M. P. de Jong, and R. Jansen, Nature (London) **462**, 491 (2009).
[20]C. H. Li, O. M. J. van 't Erve, and B. T. Jonker, Nat. Commun. **2**, 245 (2011).
[21]A. Fert and H. Jaffrès, Phys. Rev. B **64**, 184420 (2001).
[22]W. Kipferl, M. Dumm, M. Rahm, and G. Bayreuther, J. Appl. Phys. **93**, 7601 (2003).
[23]W. Wang, H. Sukegawa, and K. Inomata, Phys. Rev. B **82**, 092402 (2010).
[24]S. Sharma, S. P. Dash, H. Saito, S. Yuasa, B. J. van Wees, and R. Jansen, Phys. Rev. B **86**, 165308 (2012).
[25]K. Seeger, *Semiconductor Physics: An Introduction*, 3rd ed. (Springer-Verlag, Berlin, 1985).